UDC620.193.2:669.146.99

Corrosion Mechanisms of Zinc Alloy Coated Steel Sheets for Automobile Body Use

Kimitaka Hayashi*1 Yoichi Ito*1
Yasuhiko Miyoshi*1

Abstract:

Automobile body corrosion may be roughly classified into underfilm corrosion and perforation corrosion. These forms of corrosion have been qualitatively investigated, but not quantitatively. Among the recent study results on the corrosion mechanisms of zinc alloy coated steel sheets and the protective action of zinc alloy coatings, this paper describes: (1) the form and mechanism of underfilm corrosion in a wet environment and a wet and dry cycle environment that are widely different in corrosion tendencies, and the formulation of the corrosion rate by an underfilm coating corrosion circuit; and (2) the form and mechanism of perforation corrosion and the protective role of zinc alloy coated steel, on the basis of the results of field survey of automobiles.

1. Introduction

The corrosion protection of automobile bodies advanced toward longer durability in North America and other regions marked by severely corrosive environments. The late 1980s saw the setting of the "5-10 warranty", namely, 5-year cosmetic corrosion protection warranty and 10-year perforation corrosion protection warranty. In North America and Europe, the use of deicing salt on roadways in winter brought salt corrosion to the surface as a social problem, which in the late 1970s led to the full-fledged use of zinc alloy coated steel sheets in automobile body panels. During the intervening period, research had been actively conducted on the corrosion mechanisms of automobile body sheets with remarkable results.

Automobile body corrosion can be generally classified into two forms—underfilm corrosion and perforation corrosion[1-4]. Underfilm corrosion is a sort of cosmetic corrosion, occurs in exterior body surfaces visible to the eye, such as doors and fenders, and exhibits paint film blisters containing rust. Perforation corrosion tends to occur in steel sheet lapped joints like door inside hems.

To use zinc alloy-coated steel for protection against underfilm corrosion and perforation corrosion, it is important first to clarify the relationship of the corrosive environment with corrosion form and mechanism. Traditionally, corrosion researchers have discussed the corrosion form with the pH measurement of the underfilm corrosion product layer for underfilm corrosion[5-8], and through field survey centered on corrosion sites in steel sheet lapped joints for perforation corrosion[9]. Most of the past studies, however, have been qualitative ones without quantitatively determining the protective action of zinc alloy coatings against underfilm corrosion and perforation corrosion.

Among the past study results concerning the corrosion of zinc alloy coated steel sheets, this paper discusses: (1) the form and mechanism of underfilm corrosion in a cyclic wet and dry environment and a wet environment that drastically differ from each other in corrosion tendencies, with quantifications of an underfilm corrosion circuit and corrosion rate; and (2) the form and mechanism of perforation corrosion and the protective role of zinc alloy coated steel sheet, based on the results of field survey.

*1 Technical Development Bureau

2. Underfilm Corrosion

2.1 Form and mechanism of corrosion

2.1.1 Cyclic wet and dry environment

When specimens of zinc-15% iron alloy and zinc-11% nickel alloy coated steel sheets are painted, scribed to the steel substrate with a knife, and atmospheric exposure tested (the scribe is sprayed with 5% salt solution five times per week for accelerated corrosion), corrosion initiates from the scribe and attacks the zinc alloy coating and the steel substrate under the paint film. **Photo 1**[10] shows cross sections through painted specimens at six months of exposure near the corrosion tip. The initial corrosion layer of the coating at the tip is basic zinc hydroxychloride ($ZnCl_2 \cdot 4Zn(OH)_2$)[11]. The fact that the steel substrate just below the initial corrosion layer is not corroded indicates that the coating is sacrificially corroded at the corrosion tip before the steel substrate forms the initial corrosion layer, and protects the steel substrate[10,12,13].

When an underfilm rust sample was taken from the paint film blister near the scribe behind the corrosion tip (where the steel substrate was corroded to, increase its volume and raise the paint film) and was analyzed for composition, it was found to be composed mainly of porous iron oxides Fe_3O_4 and FeOOH. ZnO and $Zn(OH)_2$, probably the final corrosion products, were detected in some portions. The initially formed iron rust is presumed to be $Fe(OH)_2$[3,4].

Also, a pH measurement was made of the underfilm corrosion product to clarify the mechanism of underfilm corrosion. A corrosive environment similar to that of the atmospheric exposure test was established in a constant-temperature and constant-humidity cabinet. A specimen was prepared by inserting and fixing the tip of a commercial 10^{-3} m diameter minute pH electrode to the bottom surface of zinc coated steel painted in three layers. It was left to stand in the constant-temperature and constant-humidity cabinet and was investigated for the change of pH with time. The paint film of the specimen was scribed at 2×10^{-3} m from the tip of the pH electrode. The test results are shown in **Fig. 1**[11]. The pH remained near 7 for about 60 days and rose to indicate weak alkalinity when corrosion proceeded and the coating corrosion tip reached the pH electrode. This means that hydroxide ions are formed by the formation of $ZnCl_2 \cdot 4Zn(OH)_2$. As the corrosion product layer of the steel substrate reaches the tip of the pH electrode with further progress of corrosion, the pH steeply drops and indicates acidity. The pH then gradually rises and indicates that the iron rust layer is alkaline. This change in pH with the corrosion of the steel substrate is similarly confirmed from the measurements made using cold-rolled steel[4].

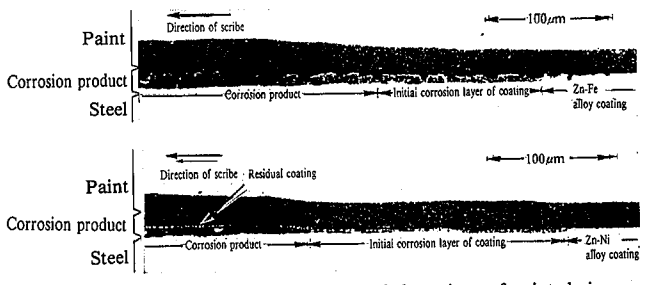

Photo 1 Cross sections through corroded portions of painted zinc alloy coated steel sheets

The reaction mechanism of underfilm corrosion may be summarized as shown in **Fig. 2**[10] from what has been discussed above. Corrosion starts at a paint film defect and creeps under the paint film. At the corrosion tip, the coating is always corroded before the steel substrate (this is called the mechanism whereby the coating is corroded before the steel substrate). $ZnCl_2 \cdot 4Zn(OH)_2$ forms in the coating in the initial stage of corrosion and finally changes to ZnO and $Zn(OH)_2$. The corrosion of the steel substrate starts with some delay after the formation of $ZnCl_2 \cdot 4Zn(OH)_2$. $Fe(OH)_2$ forms in the steel substrate in the initial stage of corrosion and eventually changes to porous Fe_3O_4 and FeOOH.

In the initial stage of coating corrosion, the coating corrosion tip serves as an anode, where zinc is dissolved and $ZnCl_2 \cdot 4Zn(OH)_2$ is formed. The cathodic reaction is an oxygen reduction reaction. The overall reaction is expressed as follows:

$$5Zn + 5H_2O + 5/2O_2 + 2Cl^- \rightarrow ZnCl_2 \cdot 4Zn(OH)_2 + 2OH^-$$

This reaction is based on the experimental fact that the pH rises with the formation of basic zinc hydroxychloride.

Basic zinc hydroxychloride is considered to finally change through $Zn(OH)_2$ to ZnO. The reaction proceeds as follows:

$$ZnCl_2 \cdot 4Zn(OH)_2 + 2OH^- \rightarrow 5Zn(OH)_2 + 2Cl^-$$

$$Zn(OH)_2 \rightarrow ZnO + H_2O$$

The above zinc corrosion reactions appear valid also from the thermodynamic study results shown in **Fig. 3**[11,14].

2.1.2 Wet environment

The pH measurement of zinc alloy coated steel specimens was made in a salt spray test environment (5% salt solution at 35°C) by methods similar to those described in the preceding section. The results are shown in **Fig. 4**[11]. The pH of the specimen steeply increased to nearly 9 with the formation of basic zinc hydroxychloride, an initial corrosion product, on the 17th day after the start of the pH measurement and then remained unchanged for

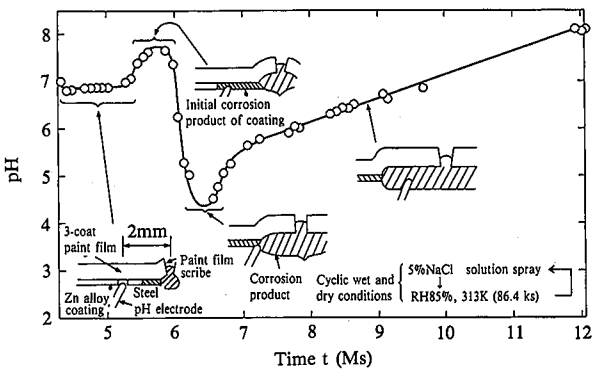

Fig. 1 Change in pH of underfilm corrosion product with time (cyclic wet and dry environment)

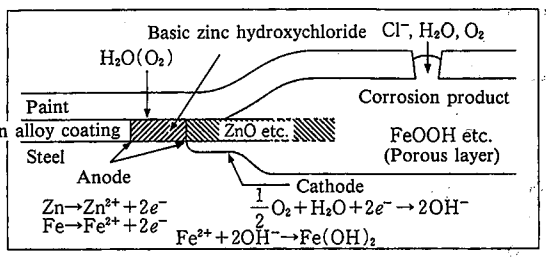

Fig. 2 Underfilm corrosion mechanism of zinc alloy coated steel sheets

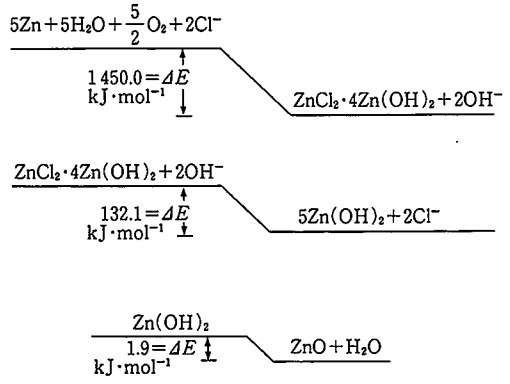

Fig. 3 Thermodynamic study of zinc corrosion

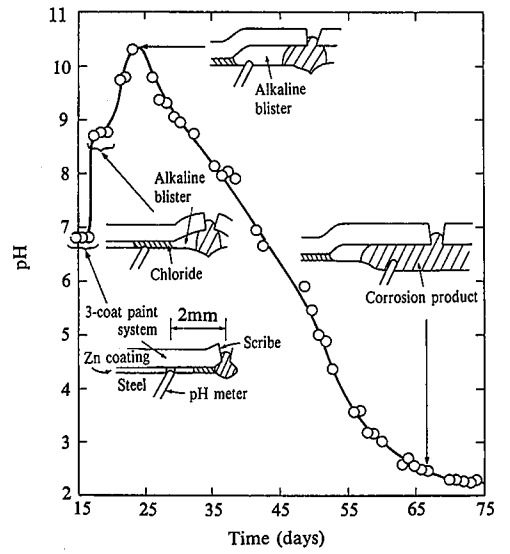

Fig. 4 Change in pH of underfilm corrosion product with time (SST environment)

several days. The pH of the specimen increased again and reached 10.4 owing to the formation of an alkaline blister on the 23rd day. After the 23rd day, the pH gradually decreased and read about 2 with the growth of the iron rust layer. **Fig. 4** schematically shows the positional relationship between the pH electrode and the rust layer at each pH level as determined by the cross-sectional observation of the specimen made simultaneously with the pH measurement.

The mechanism of underfilm corrosion in the wet environment may thus be elucidated as follows. Underfilm corrosion starts at the paint film scribe (defect) and creeps under the paint film. At the corrosion tip, the coating is corroded prior to the steel substrate. The coating forms $ZnCl_2 \cdot 4Zn(OH)_2$ in the initial stage of corrosion. As a strongly alkaline blister then forms, $ZnCl_2 \cdot 4Zn(OH)_2$ cannot remain intact but dissolves, and changes to zincate ions (ZnO_2^{2-}). This is followed by the growth of the rust layer initiated under the paint film scribe. The formation of the alkaline blister and the iron rust layer is due to the corrosion reaction of the steel substrate and is not directly related to the corrosion reaction of the coating. In this case, an oxygen reduction reaction takes place at the alkaline blister, and the dissolution reaction of the steel substrate takes place at the paint film scribe, as pointed out by Funke et al.

When the coating is initially corroded, the corrosion tip serves as anode, where zinc is dissolved and $ZnCl_2 \cdot 4Zn(OH)_2$ is formed. The cathodic reaction is an oxygen reduction reaction. The overall reaction is given by the following equation as is the case with the cyclic wet and dry environment:

$$5Zn + 5H_2O + 5/2O_2 + 2Cl^- \rightarrow ZnCl_2 \cdot 4Zn(OH)_2 + 2OH^-$$

The alkaline blister causes the reaction to proceed as follows:

$$ZnCl_2 \cdot 4Zn(OH)_2 + 12OH^- \rightarrow 5ZnO_2^{2-} + 10H_2O + 2Cl^-$$

The above zinc corrosion reactions appear valid in the light of the thermodynamic study results shown in **Fig. 5**[11].

As observed in the above-mentioned cyclic wet and dry environment, underfilm corrosion in the wet environment is characterized by the formation of $ZnCl_2 \cdot 4Zn(OH)_2$ in the initial stage of corrosion. This is a phenomenon common to all zinc alloy coated sheet products.

2.2 Quantification of zinc alloy coating corrosion circuit and corrosion rate

The actual rate of underfilm corrosion is qualitatively known to depend on the composition, weight, and corrosive environment of the zinc alloy coating. **Fig. 6**[15] and **Fig. 7**[16] show the

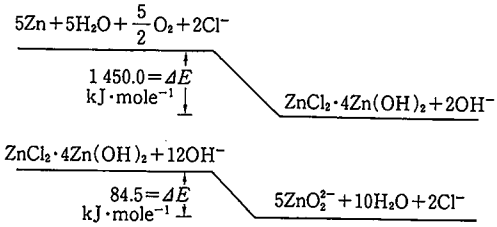

Fig. 5 Thermodynamic study of zinc corrosion

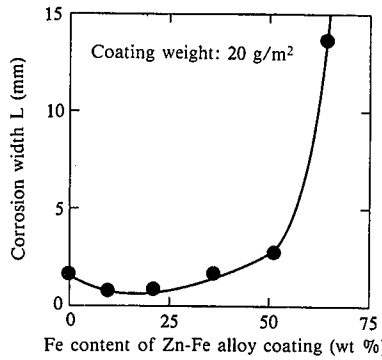

Fig. 6 Relationship between corrosion width and iron content of zinc-iron alloy coating (6-month atmospheric exposure test)

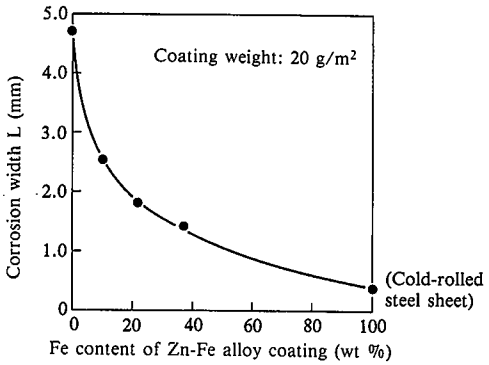

Fig. 7 Relationship between corrosion width and iron content of zinc-iron alloy coating (6-week salt spray test)

relations between the corrosion width (distance from the paint film scribe to the corrosion edge) and the composition of the zinc-iron alloy coating, respectively in the 6-month atmospheric exposure test and the 6-week salt spray test. The two figures clearly differ in terms of the corrosion width (rate). The corrosion rate varies with the type of coating, probably because of the differences in the formation of a coating corrosion microcircuit and the corrosion current through the microcircuit[17,18].

The cathodic reaction in the underfilm corrosion of the coating is regarded as an oxygen reduction reaction, but the coating corrosion circuit is not yet made clear. This is because the location of the cathode is not identified. Under two assumptions, attempts were made to derive an equation for quantifying the corrosion rate of the coating and to equally interpret relations between the corrosion rate, composition, coating weight and corrosive environment of the coating.

Assumption 1: There are two corrosion circuits, namely, a circuit on the coating (circuit having the anode and cathode on the coating) and a circuit between the coating and steel substrate (circuit having the anode on the coating and cathode on the steel substrate near the coating), at the corrosion tip, as shown in **Fig. 8**[14]. The corrosion of the coating occurs because of the coexistence of the two circuits.

Assumption 2: The corrosion of the coating proceeds with the corrosion current that is not controlled by the diffusion of oxygen.

From the above assumptions, the following equation is derived to quantify the corrosion rate of the coating:

$$\frac{L}{t}=\frac{M_{Zn}i_0^{P-P}}{nF\rho_{Zn}}\left[1+\left(\frac{l_c}{l_a}\right)\left(\frac{i_0^{P-S}}{i_0^{P-P}}\right)\frac{m_a+m_c}{m_a}\right]\frac{m_a}{m_a+m_c} \quad \cdots\cdots(1)$$

where

- i^{P-P} is density of corrosion current flowing through the corrosion circuit on the coating
- i^{P-S} is density of corrosion current flowing through corrosion circuit between the coating and the steel
- i_0^{P-P} is initial current density of the coating-coating couple
- i_0^{P-S} is initial current density of the coating-steel couple
- l_a is coating thickness
- l_c is effective steel length contributing to the formation of corrosion circuit between the coating and the steel (galvanic protection distance)
- m_a is (reciprocal of the Tafel slope for the anodic dissolution of zinc) × 2.303RT/F
- m_c is (reciprocal of the Tafel slope for the cathodic reduction of oxygen) × 2.303RT/F
- F is Faraday's constant
- n is discharge charge number of zinc

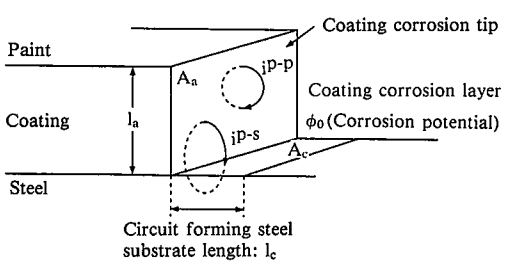

Fig. 8 Coating corrosion circuit model at corrosion tip

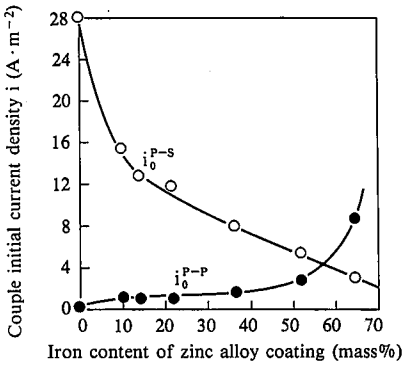

Fig. 9 Relationship between couple initial current density and iron content of zinc alloy coating

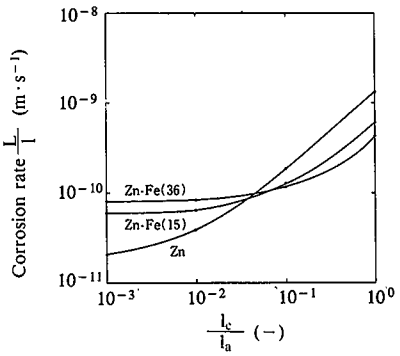

Fig. 10 Relationship between corrosion rate L/t and l_c/l_a of zinc alloy coating

- ρ_{Zn} is density of zinc
- M_{Zn} is atomic weight of zinc
- L is corrosion width (distance from the paint film scribe to the corrosion edge)
- t is corrosion time

The above equation indicates that the corrosion rate of the coating is basically expressed as a function of the couple initial current densities (i_0^{P-P}, i_0^{P-S}), and l_c/l_a[17]. The physical meaning and measuring technique of the couple initial current densities are not described in detail here, but the couple initial current densities are the values that correspond to the corrosion current that follows in each circuit and depend mainly on the composition of the zinc alloy coating as shown in **Fig. 9**[15]. The value of l_c that corresponds to the galvanic protection distance depends mainly on the corrosive environment and decreases with increasing dryness of the corrosive environment[19]. The values of m_a and m_c depend on the coating composition and other factors, strictly speaking, and are taken as constants (m_a = 3.5, m_c = 0.5) here[15]. The relationship between L/t and l_c/l_a as simulated by Eq. (1) is shown in **Fig. 10**[14]. The data of zinc alloy coated steels with the iron content ranging from 0 to 36% are given in **Fig. 10**. It is evident that the relationship between L/t and l_c/l_a varies with the coating composition and that the corrosion rate L/t decreases with decreasing l_c/l_a (increasing dryness or coating thickness).

When calculated by Eq. (1) from the measured values of L/t in **Figs. 6** and **7** where l_a is constant (2.8×10^{-6} m as converted from the coating weight of 20×10^{-3} kg/m^2), the ratio l_c/l_a is 0.05 in the atmospheric exposure test and 0.9 in the salt spray test, as shown in **Fig. 11**[15]. The value of l_c is expected to be ex-

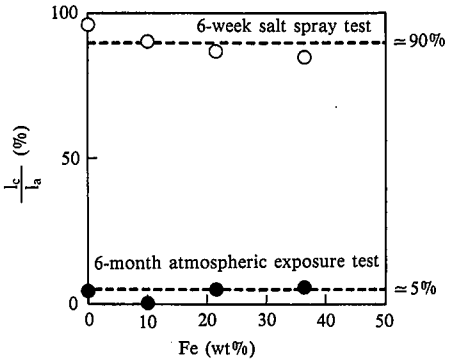

Fig. 11 Relationship between l_c/l_a and iron content of zinc alloy coating (coating weight of 20 g/m²)

tremely small in the actual service environment for corrosion-resistant steel sheet where dryness is relatively high. Under the condition of $l_c/l_a = 0.05$, it is theoretically predicted from **Fig. 10** that the corrosion rate is the lowest for low-alloy coatings with an iron content of 10 to 20%. Galvannealed steel and zinc-iron alloy coated steel in current use are designed to fall within this compositional range and are found to be optimum from a corrosion resistance point of view.

Although not discussed here, the kinetics of zinc alloy coating corrosion[20], the effect of coating weight on corrosion resistance[19], and the methods for evaluating the corrosion resistance of zinc alloy coated steel[21-23] were also studied in detail.

3. Perforation Corrosion

3.1 Corrosion form

Perforation corrosion is known to be severest in the door hems of automobiles used in North America and other salt-affected regions of the world. **Photo 2**[24-32] shows the hems of a door taken from an automobile disassembled after 10 years of use in Canada. The extent of corrosion varies according to the portion of the door. Perforation corrosion occurs not where the hem is open upward as conventionally claimed, but where the hem is closed with overlapping outer and inner panels. Another door was taken from a 4.5-year-old automobile with inner and outer door panels made of galvanized steel with a coating weight of about 90×10^{-3} kg/m² and was examined in detail by an optical microscope, electron probe microanalyzer (EPMA) and other instruments. It was found as a result that the hem portion where the coating is covered by the paint or a local rust inhibitor such as an adhesive suffers only slight corrosion[30-32]. In other words, perforation corrosion is apt to occur in bare galvanized steel surfaces without paint or inhibitor application. In this sense, the intrinsic corrosion resistance of galvanized steel in bare use governs its perforation corrosion resistance. The door hems of the 4.5-year-old automobile revealed the portions where the zinc coating was completely lost by corrosion, but the steel substrate was not corroded. The minimum field life of the 94.81×10^{-3} kg/m² zinc coating is thus estimated at 4.5 years in the door hem area. The corrosion rate in the coating thickness direction is now calculated. Since the zinc coating thickness is 0.14×10^{-6} m per 10^{-3} kg/m², the corrosion rate of the zinc coating in the field is $94.81/4.5 \times 0.14 \times 10^{-6}$ m/year $= 2.95 \times 10^{-6}$ m/year $\approx 3 \times 10^{-6}$ m/year. The field life of cold-rolled steel sheet before the onset of perforation corrosion is said to be about 2.5 years (for the sheet thickness of 0.7×10^{-3}m). When calculated from this life expectancy, the corrosion rate of cold-rolled steel sheet in the thickness direction is about 3×10^{-4} m/year[29]. The through-thickness corrosion rate ratio of the steel sheet to the zinc coating is 100:1 and shows that the corrosion rate of the zinc coating is much lower than that of the steel sheet.

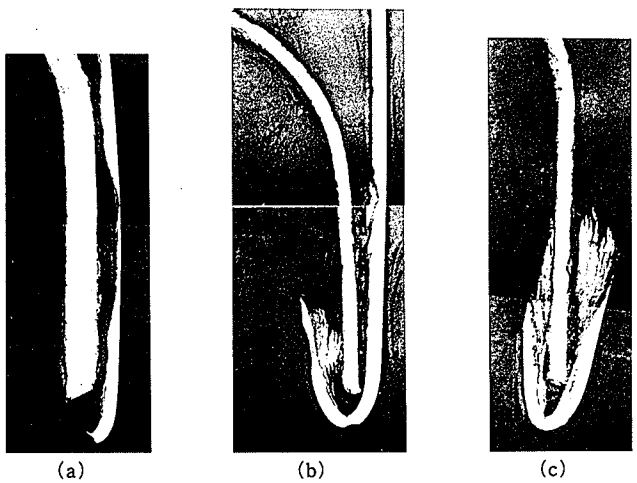

Photo 2 Door hems of automobile disassembled after 10 years of service in Canada (a, b and c are different portions of the same door)

The corrosion products in the door hem lapped joint of the 10-year-old Canadian automobile where only the inside zinc coating was corroded were examined by the X-ray diffraction technique. The formation of $ZnCl_2 \cdot 4Zn(OH)_2$ was identified. $ZnCl_2 \cdot 4Zn(OH)_2$ decreased whereas ZnO increased with aggravating corrosion. Where the steel substrate was corroded to an advanced degree, the corrosion product of the zinc coating was mostly ZnO. It is thus concluded that in the door hem flange of the automobile, the zinc in the zinc coating changed to $ZnCl_2 \cdot 4Zn(OH)_2$ in the initial corrosion of the galvanized steel and then to ZnO with the progress of corrosion[28]. This suggests that the perforation corrosion of galvanized steel can occur as indicated by the thermodynamic study shown in **Fig. 3**.

To interpret the above-mentioned corrosion phenomena inside the door hem, the next section studies the corrosion characteristics of zinc and the electrochemical coupling behavior of zinc and iron, and clarifies the role of the zinc coating against perforation corrosion.

3.2 Role of zinc coating against perforation corrosion

Salt solutions were adjusted to different pH levels using HCl and NaOH, and a 50 cm² pure zinc specimen was immersed in 100 cm³ of each solution thus prepared and observed for corrosion. (The corrosion products were identified, and the change in the pH of the solution was measured.) The corrosion characteristics of zinc were studied from the results obtained. As can be seen from **Fig. 12**, $ZnCl_2 \cdot 4Zn(OH)_2$ and ZnO are formed as corrosion products of zinc in solutions with a NaCl concentration of 1% or more. This finding indicates that the door hem was exposed to an environment containing 1% or more NaCl. As shown in **Fig. 13**, solutions with an initial pH of 5 to 12 changed to pH of about 9 on the 10th day with the dissolution of zinc in the solution (containing no NaCl). The dissolution of zinc is considered effective in stabilizing the pH of the solution.

Sample	Composition	NaCl (wt%)							
		0	10^{-3}	10^{-2}	10^{-1}	1	5	10	20
Sample surface	Zn	←							→
	$ZnCl_2 \cdot 4Zn(OH)_2$					←			→
	$Zn(OH)_2$	←					→		
	ZnO	←							→
Solution residue	$ZnCl_2 \cdot 4Zn(OH)_2$								
	$Zn(OH)_2$								
	ZnO	←					→		

Fig. 12 Relationship between zinc corrosion products and NaCl concentration

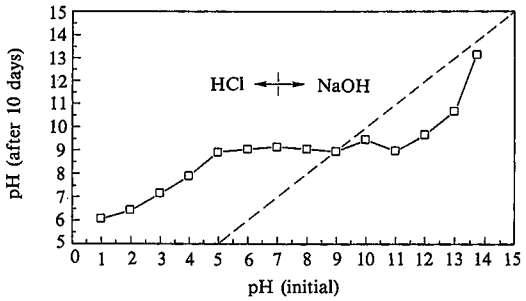

Fig. 13 Change in pH with dissolution of zinc

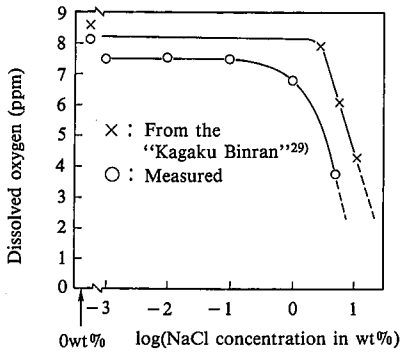

Fig. 14 NaCl concentration dependence of amount of dissolved oxygen (at 25°C)

This pH value approximately agrees with the pH of 8.5 or 9 obtained from the solubility product K_p of $Zn(OH)_2$ or $ZnCl_2 \cdot 4Zn(OH)_2$.

The electrochemical couple behavior of an outer galvanized steel panel and an inner cold-rolled steel panel in a door hem (or of the inside zinc coating and exposed steel substrate of the outer panel) was investigated as described below.

The amount of oxygen dissolved in NaCl solutions of various concentrations was measured first. As shown in **Fig. 14**, the dissolved oxygen measurements are close to those presented in Kagaku Binran ("Handbook of Chemistry" in Japanese)[29]. This attests to the extremely high reliability of the dissolved oxygen measurements. When obtained from the measured amount of oxygen dissolved in a 5% NaCl solution, for example, according to Fick's first law, the oxygen diffusion limiting current density in a still bath is about 100×10^{-2} A/m^2. The sacrificial protection range of the hem flange area as determined from this value is shown in **Fig. 15**. The rest potential difference between the outer panel inside zinc coating and the cold-rolled steel inner panel was taken as the potential difference between the outer and

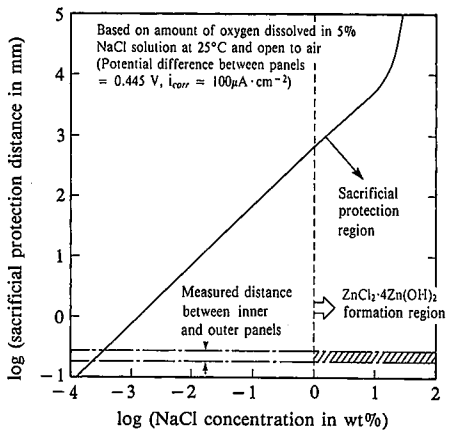

Fig. 15 Sacrificial protection range in automobile door hem flange

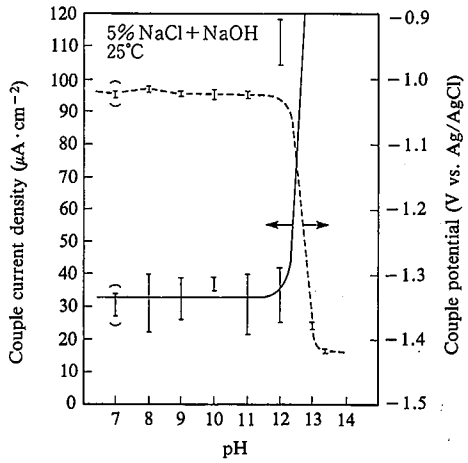

Fig. 16 Couple behavior of zinc and iron

inner panels. The values of equivalent electrical conductivity given in Kagaku Binran[29] were used as equivalent electrical conductivity in NaCl solutions. The distance between the inner and outer panels of doors in North American automobiles in the field was measured to be about 180 to 200 $\times 10^{-6}$ m. Assuming that a NaCl solution with a NaCl concentration of 1% or more is present in the hem flange area taking into consideration the existence of $ZnCl_2 \cdot 4Zn(OH)_2$ as corrosion product, it is suggested that sacrificial protection could well occur between the outer and inner panels as indicated by the shaded region of **Fig. 15**. The electrochemical couple behavior of zinc (pure zinc sheet) with a measuring area of 1 cm^2 and iron (cold-rolled steel) in a 5% NaCl solution (100 cm^3) adjusted to any desired pH by NaOH was investigated (the mixed potential and current were measured). **Fig. 16** shows the relationship between the couple current and the pH. The couple current is small and 20 to 40 $\times 10^{-2}$ A/m^2 in the pH range of 7 to 12. This value is smaller than the 100 $\times 10^{-2}$ A/m^2 presumed from the amount of dissolved oxygen. A sharp increase in the couple current is observed in the pH range of over 12. The rest potential in the couple condition is slightly less noble than -1 V, is practically constant in the pH range of 7 to 12, and suddenly becomes less noble as the pH exceeds 12. These results are presented on a potential-pH diagram in **Fig. 17**. The measured values (indicated by solid circles) are the aver-

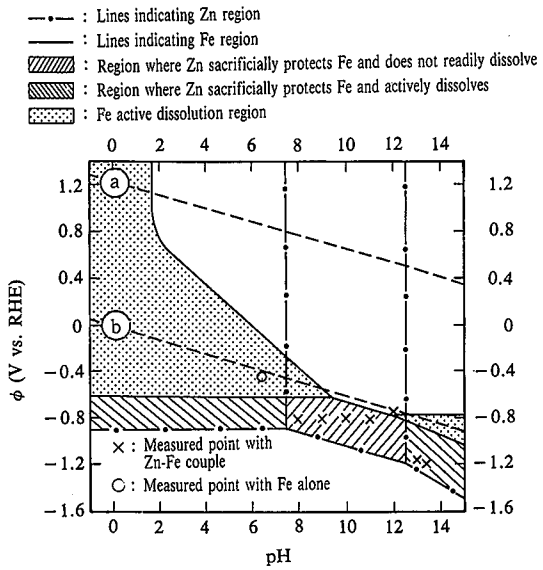

Fig. 17 Potential-pH diagram of zinc and iron

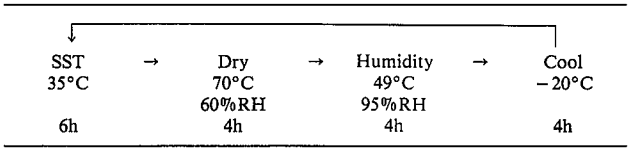

Fig. 18 Cyclic corrosion test condition

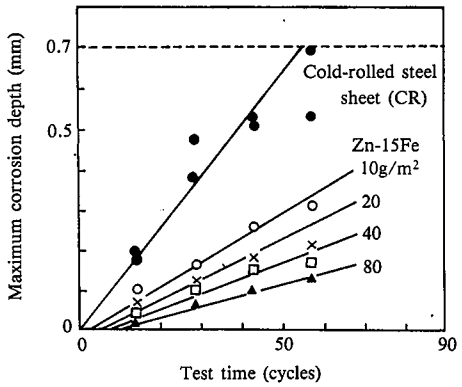

Fig. 19 Results of cyclic perforation corrosion test with lapped flat steel sheet specimens

age values of the potentials shown in **Fig. 16**. The measured values of the rest potential for iron alone (indicated by the letter ×) are those measured in a 5%NaCl solution open to air. The measured data points for iron alone are located in the iron active dissolution region. In the pH region of neutrality to weak alkalinity, the iron-zinc couple is expected to make the rest potential less noble and to keep the iron and zinc in the immunity region and the passivation region, respectively. Since the couple current is smaller than the oxygen diffusion limiting current in the pH range of neutrality to weak alkalinity, the formation of a protective corrosion product film is considered responsible as reported by Hisamatsu[33]. The results of the field survey and laboratory research discussed in the preceding section indicate that $ZnCl_2 \cdot 4Zn(OH)_2$ may be the protective corrosion product.

From what has been discussed, the role[34] of zinc coating in protecting the steel sheet lap in the hem against perforation corrosion may be considered as follows. The zinc coating on the steel sheet galvanically protects the steel substrate. It also dissolves to keep the environment stably alkaline and inhibits its own dissolution by forming a protective film of $ZnCl_2 \cdot 4Zn(OH)_2$ on its surface. It is thus effective against perforation corrosion. This may be interpreted to indicate that the presence of $ZnCl_2 \cdot 4Zn(OH)_2$ as corrosion product as indicated in the preceding section makes the ratio of cold-rolled steel to zinc coating 100:1 in terms of corrosion rate.

In **Fig. 18**, the cyclic corrosion test procedure is shown as the method for simulating the corrosion of the hem. The evaluation results of lapped test specimens[22] in the cyclic corrosion test demonstrate the effect of coating weight in resisting perforation corrosion, as shown in **Fig. 19**[30]. The straight lines for the zinc-iron alloy coated steel do not pass through the origin, which points to the presence of a certain incubation period. Since the incubation period increases with increasing coating weight, the zinc coating alone is considered to be corroded during the incubation period. After the incubation period, the straight lines start to rise. The slope of the straight line is smaller for the zinc-iron alloy coated steel than for the cold-rolled steel and decreases with increasing coating weight. This indicates that the corrosion behavior of the steel substrate after the loss of the zinc-iron alloy coating is different from that of the cold-rolled steel. This tendency is not observed with flat steel sheets. When lapped steel sheet specimens are opened and observed, corrosion is locally caused, and portions where the steel substrate is corroded are present together with those where the coating remains. Because the specimens are those of lapped steel sheets, the zinc-containing corrosion products do not readily run out of the hem, but remain covering the steel sheet surface. This is attributable to the galvanic protective action of the adjoining zinc coating and the protective action of corrosion products, as described above. Localized corrosion also occurs in actual automobiles as shown in **Photo 2**. Since the corrosion products are not considered to easily run out of the hem, it is presumed that a phenomenon similar to that observed with the lapped steel sheet specimens is also caused in the hem.

3.3 Corrosion mechanism

Disassembling investigation of field automobiles[24-32,35,36] yielded the following findings: 1) Perforation proceeded from the inside to the outside of the hem in one case, and the corrosion initiated at the hem edge proceeded into the hem in another case. The former condition is likely to occur when the adhesive is not properly applied, and the latter when the adhesive is properly applied but the sealer is not. 2) The outer panel is corroded more severely than the inner panel. 3) When the corrosion products are accumulated in the hem, their volume expansion widens the gap of the hem.

The mechanism of perforation corrosion may thus be elucidated as follows. Corrosion factors, such as oxygen, water, chloride ions and mud, enter the inside of the door through the window or the like, or are supplied through the corroded portion of the hem edge to the hem. If local inhibitors are improperly applied, are degraded with time, or not tightly applied to the steel sheet, the zinc coating starts to corrode. The inside of the hem

is practically unpainted and is susceptible to corrosion. The air temperature difference between the inside and outside of the hem facilitates dew condensation inside the hem and causes the corrosion to continue inside the hem even after the disappearance of rainwater or other water introduced into the hem. This tendency is particularly pronounced on the outer panel, so that the outer panel suffers heavier corrosion than the inner panel. As the zinc coating is corroded, the underlying steel substrate starts to corrode. When the corrosion products of the steel substrate are formed, their volume expansion widens the gap of the hem, promotes the supply of corrosion factors, and accelerates the corrosion of the hem. Perforation proceeds from the inside to the outside of the hem. Once holes are opened, corrosion factors are supplied also through the open holes to further accelerate the corrosion of the hem.

Local inhibitors can be effectively applied against perforation corrosion. Given the difficulty of properly applying local inhibitors, however, the use of zinc alloy coated steel will continue to be an essential solution to the corrosion problem.

4. Conclusions

Work has rapidly advanced on the research and development of zinc alloy coated steel sheets for the corrosion protection of automobile bodies, and various zinc alloy coated steel products are now used in this automotive application. Given the future development of new zinc alloy coated steels and use of existing coated sheet products in right applications, it is considered essential to clarify the corrosion mechanism and protective role of coatings. Recent research results have been presented above concerning the corrosion mechanisms of zinc alloy coated steels and the protective action of zinc alloy coatings.

References

1) Miyoshi, Y.: Corrosion Engineering. 35 (1), 38 (1986)
2) Miyoshi, Y.: 138th and 139th Nishiyama Memorial Lecture, Tokyo and Osaka, 1991, ISIJ, p.139-164
3) Hayashi, K.: J. Adhesion Society Japan. 26 (5), 194 (1990)
4) Hayashi, K. et al.: Tetsu-to-Hagané. 76 (8), 1309 (1990)
5) Jossic, T. et al.: Corrosion 88. No. 355, NACE, 1988
6) Miki, K. et al.: Tetsu-to-Hagané. 72 (9), 1090 (1986)
7) Ikeda, K. et al.: Tetsu-to-Hagané. 73, S1161 (1987)
8) Nishimura, K. et al.: Tetsu-to-Hagané. 73, 892 (1987)
9) Vos. E.: Programme quebecois anti-roulle. Delplace Ltd. Montreal, 1979
10) Hayashi, K. et al.: Tetsu-to-Hagané. 76 (8), 1317 (1990)
11) Hayashi, K. et al.: Tetsu-to-Hagané. 78 (10), 1577 (1992)
12) Hayashi, K. et al.: Tetsu-to-Hagané. 76 (9), 1496 (1990)
13) Hayashi, K.: J. Mater. Product Tech. 6 (1), 9 (1991)
14) Hayashi, K.: Bull. Jpn. Inst. Met. 32 (2), 86 (1993)
15) Hayashi, K. et al.: Tetsu-to-Hagané. 77 (10), 1695 (1991)
16) Hayashi, K. et al.: Tetsu-to-Hagané. 77 (10), 1688 (1991)
17) Hayashi, K. et al.: Tetsu-to-Hagané. 77 (7), 1122 (1991)
18) Ito, Y. et al.: Tetsu-to-Hagané. 77 (7), 1138 (1991)
19) Hayashi, K. et al.: Tetsu-to-Hagané. 78 (1), 127 (1992)
20) Hayashi, K. et al.: Tetsu-to-Hagané. 78 (4), 601 (1992)
21) Miyoshi, Y. et al.: SAE 820334. 1982
22) Miyoshi, Y. et al.: SAE 840210. 1984
23) Miyoshi, Y. et al.: SAE 850007. 1985
24) Ito, Y. et al.: SAE 892580. 1989
25) Miyoshi, Y.: ISIJ International. 31 (1), 1 (1991)
26) Miyoshi, Y.: ISIJ International. 31 (2), 122 (1991)
27) Miyoshi, Y.: Journal of JSAE. 45 (9), 5 (1991)
28) Hayashi, K. et al.: SAE 912279. 1991
29) Chemical Society of Japan: Kagaku Binran ("Handbook of Chemistry" in Japanese). Second Edition. Volume II. Fundamentals. p. 770-773
30) Miyoshi, K. et al.: Proc. GALVATECH '92, Amsterdam, September 1992, CRM, p.528
31) Miyoshi, Y. et al.: Shinnitettsu Giho. (347), 16 (1992)
32) Miyoshi, Y. et al.: Nippon Steel Tech. Rep. (57), 16 (1993)
33) Hisamatsu, T.: Tetsu-to-Hagané. 71 (10), 1719 (1985)
34) Hayashi, K. et al.: Proc. of 39th Corrosion and Corrosion Prevention Meeting, 1992, p.443
35) Miyoshi, Y.: AESF SUR/FIN'93, Anaheim, 1993.6, p.1
36) Nakazawa, M. et al.: SAE 932367. 1993